Chemical Science

rsc.li/chemical-science

ROYAL SOCIETY
OF CHEMISTRY

EDGE ARTICLE
Jochen Autschbach, Ning Chen *et al.*
$ThC_2@C_{82}$ *versus* $Th@C_{84}$: unexpected formation of
triangular thorium carbide cluster inside fullerenes

Check for updates

ThC₂@C₈₂ *versus* Th@C₈₄: unexpected formation of triangular thorium carbide cluster inside fullerenes†

Yi Shen, ‡[a] Xiaojuan Yu, ‡[b] Qingyu Meng,[a] Yang-Rong Yao [a]
Jochen Autschbach *[b] and Ning Chen *[a]

Synthesis of the first thorium-containing clusterfullerenes, $ThC_2@C_s(6)-C_{82}$ and $ThC_2@C_2(5)-C_{82}$, is reported. These two novel actinide fullerene compounds were characterized by mass spectrometry, single-crystal X-ray diffraction crystallography, UV−vis−NIR spectroscopy, and theoretical calculations. Crystallographic studies reveal that the encapsulated ThC_2 clusters in both $C_s(6)-C_{82}$ and $C_2(5)-C_{82}$ feature a novel bonding structure with one thorium metal center connected by a C≡C unit, forming an isosceles triangular configuration, which has not been hitherto observed for endohedral fullerenes or for solid phase thorium carbides. Electronic structure calculations assign a formal electronic structure of $[Th^{4+}(C_2)^{2-}]^{2+}@[C_{82}]^{2-}$, with pronounced donation bonding from $(C_2)^{2-}$ to Th^{4+}, secondary backbonding from the fullerene to thorium and Th−C double bond character in both compounds. This work presents a new family of endohedral fullerenes, $MC_2@C_{2n-2}$, being unexpected isomers of MC_{2n}, and provides broader understanding of thorium bonding.

Introduction

Fullerenes are known for their ability to encapsulate clusters, which results in the formation of unique host–guest molecular compounds—endohedral clusterfullerenes.[1–3] The unique interaction and mutual stabilization between the metal-containing clusters and fullerenes gave rise to fascinating electronic structures and potential applications of these compounds.[4–7] To date, most lanthanides have been encapsulated in fullerene cages.[8] Our recent research showed that novel actinide clusters can also be captured and stabilized by fullerene cages, such as $U_2C@I_h(7)-C_{80}$, $U_2C_2@I_h(7)-C_{80}$, or $UCN@C_{82}$.[9–11] These systems exhibit substantially different electronic structures compared to known lanthanide-based analogs. In particular, the encapsulated uranium clusters reveal bonding properties that have never been observed in conventional uranium compounds. Thus, the exploration of novel actinide cluster fullerenes will not only expand the scope

of endohedral fullerenes, but also have significance regarding the understanding of fundamental actinide chemistry. However, all of the actinide cluster fullerenes discovered thus far were based on uranium; other actinide cluster fullerenes have yet to be explored.[12]

Thorium is arguably the new frontier of nuclear energy.[13] Attempts have been made to synthesize and characterize thorium compounds for use as potential fuels in advanced reactors. Recently, thorium carbides have attracted increasing attention because these compounds are suitable for high-burnup and high-temperature operations with increased "margin to melting" in the framework of modern nuclear systems.[14] Many advantages of thorium carbides, such as high melting points, corrosion resistivity, low thermal expansion coefficients and high thermal conductivity, have been reported in recent research.[15,16] Therefore, understanding the behavior and properties of thorium carbides is essential to explore their potential application as nuclear reactor fuel materials.[17,18]

Thorium carbides (ThC_n, $n = 1–6$) have been detected in vapors above solid carbides or metal alloys in graphite systems, and partial pressures of thorium carbides were measured by mass spectrometry.[19–22] Thorium dicarbide (ThC_2), as the main type of stoichiometric thorium carbides, exists in polymorphic modifications at ambient pressure.[16,23–25] However, the structural and electronic properties of ThC_2 have only been studied by theoretical calculations.[18,23,26] Thus far, the molecular structure of ThC_2 has not been observed in the condensed phase.

On the other hand, carbide cluster fullerenes (CCFs) are an important branch of endohedral cluster fullerenes and have

[a]College of Chemistry, Chemical Engineering and Materials Science, State Key Laboratory of Radiation Medicine and Protection, Soochow University, Suzhou, Jiangsu 215123, P. R. China. E-mail: chenning@suda.edu.cn

[b]Department of Chemistry, University at Buffalo, State University of New York, Buffalo, NY 14260-3000, USA

‡ These authors contributed equally to this work.

been extensively investigated in the past two decades.[12] The first reported CCF is $Sc_2C_2@D_{2d}(23)$–C_{84}, initially assigned as a di-metallofullerene (EMF), $Sc_2@C_{86}$.[27] This discovery confirmed that the composition M_2C_{2n} could exist as M_2C_{2n} or as $M_2C_2@C_{2n-2}$. Subsequent studies revealed a large family of CCFs with variable M_2C_2 clusters encapsulated inside different fullerene cages, such as $Sc_2C_2@C_{2n}$,[28–30] $Gd_2C_2@C_{2n}$,[31] $Lu_2C_2@C_{2n}$[32] et al.[2] In addition, composition Sc_3C_{82} was also reassigned as $Sc_3C_2@I_h$–C_{80}.[33] Up to now, a large variety of CCFs entrapping multiple (2–4) metal atoms have been reported. However, monometallic carbide cluster fullerenes have not been yet available and whether $M@C_{2n}$ can exit as as MC_{2n} or as $MC_2@C_{2n-2}$ has yet to be explored.

Herein, we report the first thorium-based cluster fullerenes, namely, $ThC_2@C_s(6)$–C_{82} and $ThC_2@C_2(5)$–C_{82}. Crystallographic studies reveal that, these two actinide endohedral fullerenes, initially assigned as isomers of $Th@C_{84}$, are in fact thorium-based cluster fullerenes which contains a unique mononuclear thorium carbide cluster. Theoretical analyses confirm that $ThC_2@C_s(6)$–C_{82} and $ThC_2@C_2(5)$–C_{82} can be described by a formal two-electron transfer from the ThC_2 cluster to the C_{82} cage, which results in formal closed-shell electronic structures $[Th^{4+}(C_2)^{2-}]^{2+}@[C_{82}]^{2-}$.

Results and discussion

Synthesis and isolation of $ThC_2@C_s(6)$–C_{82} and $ThC_2@C_2(5)$–C_{82}

Thorium-based endohedral metallofullerenes were synthesized by a modified Krätschmer–Huffman DC arc discharge method. Graphite rods packed with U_3O_8/ThO_2 and graphite powder (molar ratio of $U : Th : C = 1 : 1 : 30$) were vaporized in the arcing chamber under a 200 Torr He atmosphere. The resulting soot was then collected and extracted with CS_2 for 12 h. A series of thorium-containing endohedral metallofullerenes were generated from this process (Fig. S2†) and in this work, two novel isomers(I,II) of ThC_{84} (later assigned as $ThC_2@C_s(6)$–C_{82} and $ThC_2@C_2(5)$–C_{82}) were isolated by a multistage high-performance liquid chromatography (HPLC) separation process (Fig. S1†). The purity of the isolated compounds was confirmed by positive-ion-mode matrix-assisted laser/desorption ionization time-of-flight mass spectrometry (MALDI-TOF/MS), as shown in Fig. 1. The mass spectra of $ThC_2@C_s(6)$–C_{82} and $ThC_2@C_2(5)$–C_{82} show peaks at m/z = 1240.196 and 1240.204. In addition, the experimental isotopic distributions of the two samples agree well with theoretical predictions.

Molecular and electronic structures of $ThC_2@C_s(6)$–$C_{82}\cdot[Ni^{II}OEP]$ and $ThC_2@C_2(5)$–$C_{82}\cdot[Ni^{II}OEP]$

Two black block cocrystals were obtained by slow diffusion of $Ni^{II}(OEP)$ (OEP = 2,3,7,8,12,13,17,18-octaethylporphin dianion) in benzene into a CS_2 solution of the corresponding compounds. $Ni^{II}(OEP)$ was used to hinder rotation of fullerene molecules in the co-crystal. The molecular structures of $ThC_2@C_s(6)$-$C_{82}\cdot[Ni^{II}OEP]$ and $ThC_2@C_2(5)$-$C_{82}\cdot[Ni^{II}OEP]$ were
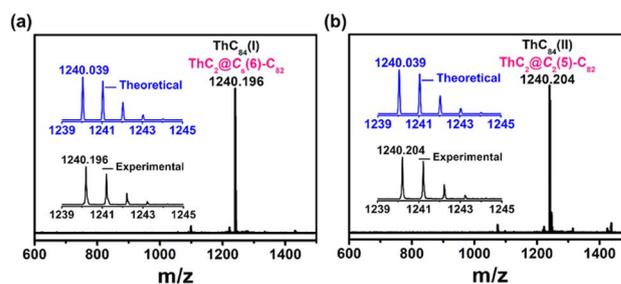

Fig. 1 Positive-ion mode MALDI-TOF mass spectra of purified (a) $ThC_2@C_s(6)$–C_{82} and (b) $ThC_2@C_2(5)$–C_{82}. The insets show the experimental and theoretical isotopic distribution for compounds.

determined by single-crystal X-ray diffraction analysis, excluding other molecular structures with the same molecular weight, such as Th-based mono-metallofullerenes, $Th@C_{84}$ isomers. The shortest Ni-cage distance was measured as 2.846(104) and 2.855(115) Å for $ThC_2@C_s(6)$–$C_{82}\cdot[Ni^{II}OEP]$ and $ThC_2@C_2(5)$–$C_{82}\cdot[Ni^{II}OEP]$, indicating a strong π–π interaction between $ThC_2@C_{82}$ and $Ni^{II}(OEP)$. Both $ThC_2@C_s(6)$–$C_{82}\cdot[Ni^{II}OEP]$ and $ThC_2@C_2(5)$–$C_{82}\cdot[Ni^{II}OEP]$ were solved in the monoclinic space group C2/m.

The whole molecule of $ThC_2@C_s(6)$–C_{82}, including the fullerene cage and the encapsulated cluster, shows two equivalent orientations with the same occupancy of 0.5, which is common in many analogous metallofullerene/$Ni^{II}(OEP)$ cocrystal systems.[1] The encapsulated Th ion shows only slight disorder with a total occupancy of 0.5 for the three disordered sites Th1–Th3. Th1 is assigned as the major Th site, as it has a much higher occupancy of 0.418 compared to those of the other two sites (0.0489 and 0.0326 for Th2 and Th3, respectively). Furthermore, Th1A, Th2A and Th3A are also generated via their mirror-related counterparts, Th1, Th2 and Th3, due to the same crystallographic mirror plane. Further structural analysis shows that Th1 is situated on the symmetry plane of the $C_s(6)$–C_{82} cage, while Th1A is located away from the symmetry plane (Fig. S4†). The density functional theory (DFT) calculation results also suggest that the Th1 site is approximately 13 kcal mol^{-1} lower in energy for all functionals than Th1A (Table S2†). In addition, previous studies suggest that the metal ion prefers to remain symmetrically aligned with interacting motifs that share one of the symmetry planes with the fullerene containing mirror planes.[34] Therefore, we assign Th1 as the optimal position of $ThC_2@C_s(6)$–C_{82} (Fig. 2a).

The crystallographic results of $ThC_2@C_2(5)$–C_{82} also show two orientations of the fullerene molecule with equal occupancy of 0.5. These two orientations are related by the molecular crystallographic mirror. The Th1 site is the major Th position for $ThC_2@C_2(5)$–C_{82}, with a fractional occupancy of 0.281. Th1A has the same occupancy of 0.281 and is symmetrical with Th1 through a crystallographic mirror. The rest of the minor sites are displayed in Fig. S3(b).† Th1 is located beneath the corresponding hexagon, with the shortest metal-cage distances of 2.542(12) Å (Th1–C3) and 2.589(13) Å (Th1–C2). Its mirror-related counterpart, Th1A, on the other hand, has the closest
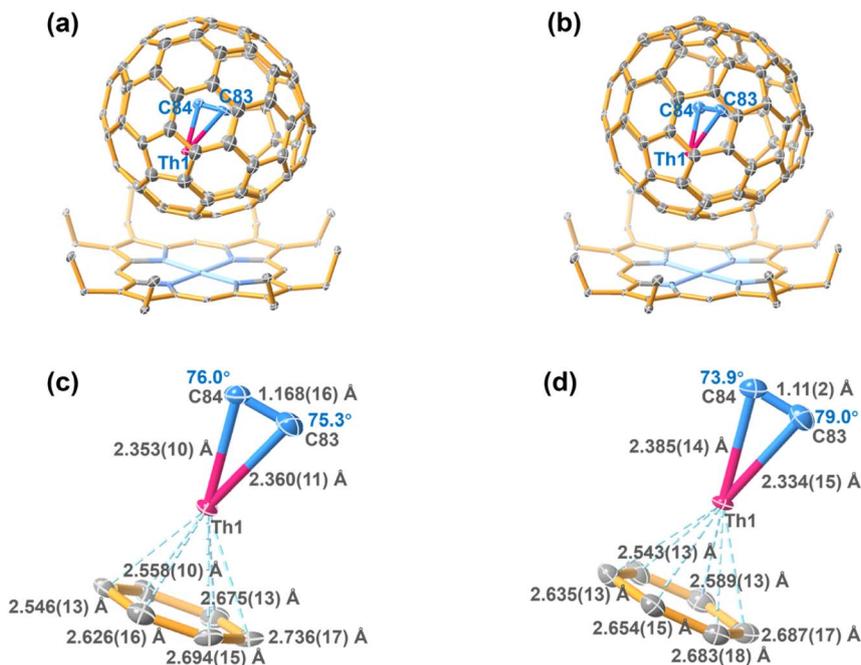
Fig. 2 ORTEP drawing of $ThC_2@C_s(6)-C_{82}\cdot[Ni^{II}OEP]$ (a) and $ThC_2@C_2(5)-C_{82}\cdot[Ni^{II}OEP]$ (b) with 20% thermal ellipsoids. Only the predominant Th (Th1) sites are shown. For clarity, the solvent molecules and minor metal sites (Fig. S3†) are omitted. Fragment view showing the interaction of the ThC_2 clusters with the closest aromatic ring fragments of the $C_s(6)-C_{82}$ cage (c) and $C_2(5)-C_{82}$ cage (d).

metal-cage of 2.475(13) (Th1A–C33) and 2.576(14) (Th1A–C55) Å, respectively (Fig. S5†). Thus, in this case, neither Th1 nor Th1A can be assigned as the optimal site only by crystallographic analysis, and their metal-cage distances are very similar. Therefore, theoretical calculations were employed to further determine the optimized position of the encapsulated ThC_2 cluster relative to the selected cage orientation. The results show that the Th1 site has a lower energy than the Th1A site for $ThC_2@C_2(5)-C_{82}$ (Table S2†). Thus, the optimal ThC_2 cluster orientation can be accurately determined, as shown in Fig. 2b.

As shown in Fig. 2c and d, the Th–C distances are 2.360(11)/ 2.353(10) Å for $ThC_2@C_s(6)-C_{82}$ and 2.334(15)/2.385(14) Å for $ThC_2@C_2(5)-C_{82}$, which are significantly shorter than the Th–C single bonds in thorium-based organometallic complexes (2.471–2.892 Å),[35,36] as shown in Table 1. Moreover, for the encapsulated cluster ThC_2, the C–C distances from the X-ray diffraction are 1.168(16) Å and 1.11(2) Å in the $C_s(6)-C_{82}$ and $C_2(5)-C_{82}$ cages, respectively, as shown in Table S3.† These C–C bonds can be assigned as triple bonds, but they are approximately 0.1 Å shorter than the optimized distances obtained by theoretical calculations (1.252 and 1.251 Å, respectively) of the isolated cluster fullerenes. The unusual phenomenon of shrinking C–C bonds inside fullerene cages has also been observed for metal carbide cluster fullerenes such as $Sc_2C_2@$-$D_{3h}(14\,246)-C_{74}$, $Ga_2C_2@D_3(85)-C_{92}$ and $U_2C_2@D_{3h}(5)-C_{78}$, in which the X-ray crystallographically determined C–C bond lengths (1.049(17) Å,[37] 1.04(2) Å (ref. 38) and 1.127(18) Å (ref. 10) respectively) are also notably shorter than the C–C triple bonds in alkyne compounds (1.21 Å). In addition, as shown in Fig. 2c

Table 1 Comparison of Th–C distances in $ThC_2@C_{82}$ and thorium-based organometallic complexes

system	Th···C distance (Å)	Ref.
$ThC_2@C_s(6)-C_{82}$	2.360(11)/2.353(10)	This work
$ThC_2@C_2(5)-C_{82}$	2.334(15)/2.385(14)	This work
$[1,3-(SiMe_3)_2C_3H_3]_4Th$	2.617(5)–2.892(5)	35
$[1-(SiMe_3)C_3H_4]_4Th$	2.679(3)–2.806(3)	35
$(C_5Me_5)_2ThMe_2$	2.471(8)/2.478(9)	36
$(C_5Me_5)_2Th(CH_2Ph)_2$	2.552(7)/2.551(7)	36

and d, the metal–C_{cage} distances are 2.546(13)–2.736(17) Å for $ThC_2@C_s(6)-C_{82}$ and 2.543(13)–2.687(17) Å for $ThC_2@C_2(5)-C_{82}$, which agree well with the theoretical calculations (Table S3†) (2.606–2.814 Å for $ThC_2@C_s(6)-C_{82}$ and 2.635–2.686 Å for $ThC_2@C_2(5)-C_{82}$). These distances are similar to the Th–Cp(cent) distances in organometallic compounds; for example, the Th–Cp(cent) distances are 2.532(4)–2.649(8) Å in actinide phosphinidene metallocene (Cp = cyclopentadienyl ring).[39,40] This result suggests that the coordination interaction between Th and the fullerene cage may be similar to that between Th and the cyclopentadienyl group in organometallic compounds.

The ThC_2 cluster in $C_s(6)-C_{82}$ features two almost identical Th–C distances, 2.360(11) and 2.353(10) Å, respectively, leading to an isosceles triangular configuration. ThC_2 in $C_2(5)-C_{82}$ has a similar but slightly distorted isosceles triangular configuration, with a Th–C bond length difference of 0.05 Å. Note that the metal–C_{cage} distances in the two $ThC_2@C_{82}$ isomers, as mentioned already, are also somewhat different [2.546(13)–

2.736(17) Å for $ThC_2@C_s(6)$–C_{82} and 2.543(13)–2.687(17) Å for $ThC_2@C_2(5)$–C_{82}]. This result suggests that the variable isomeric cage structure has a slight impact on the interaction between Th and cage carbon, which likely results in differences in the ThC_2 cluster configurations inside the two C_{82} cage isomers.

The symmetric isosceles triangular structure configuration of the ThC_2 cluster encapsulated in either $C_2(5)$–C_{82} or $C_s(6)$–C_{82} is similar to a previously reported theoretically optimized structure of the ThC_2 molecule:[18] Kovacs and coworkers predicted that, for neutral ThC_2, the symmetric triangular arrangement is much more stable than alternate linear or asymmetric triangular conformations.[18,41] The Th–C distance in the symmetric triangular isolated ThC_2 molecule obtained in the previous calculations is 2.281 Å,[18,41] which is shorter than the experimentally obtained Th–C bond length for $ThC_2@C_{82}$ (2.360(11)/2.353(10) Å for $ThC_2@C_s(6)$–C_{82} and 2.334(15)/2.385(14) Å for $ThC_2@C_2(5)$–C_{82}). The variability of the Th–C distance may be rationalized by the fact that the coordination bonding between the Th and C_2 moiety in $ThC_2@C_{82}$ is weakened by the coordination interaction between Th and the fullerene cage, as discussed later.

A closer look at the symmetric structure of $ThC_2@C_s(6)$–C_{82} shows that, although the encapsulated ThC_2 can have many possible orientations relative to the cage, both the metal atom, Th1, and the cluster, ThC_2, are located right on the symmetry plane. Further analysis of the crystallographic data of other mononuclear cluster fullerene-containing symmetry planes, such as $MCN@C_s(6)$–C_{82} (M = U, Y and Dy), $MCN@C_{2v}(19\,138)$–C_{76} (M = Tb, Lu and Y), $DyCN@C_{2v}(9)$–C_{82} and $DyCN@C_{2v}(17)$–C_{84}, as show in Fig. 4 suggests that the encapsulated mononuclear clusters are all located on the mirror planes of fullerene cages (see Fig. 3).[5,11,42–45] Previous studies of monometallic fullerenes (only one metal ion inside the cage) have found that in fullerene cages containing symmetry planes, the metal prefers to occupy a symmetric arrangement with respect to the interacting motifs, which share one of their symmetry planes with the fullerene.[34] This observation further suggests that the endohedral mononuclear cluster also prefers to share
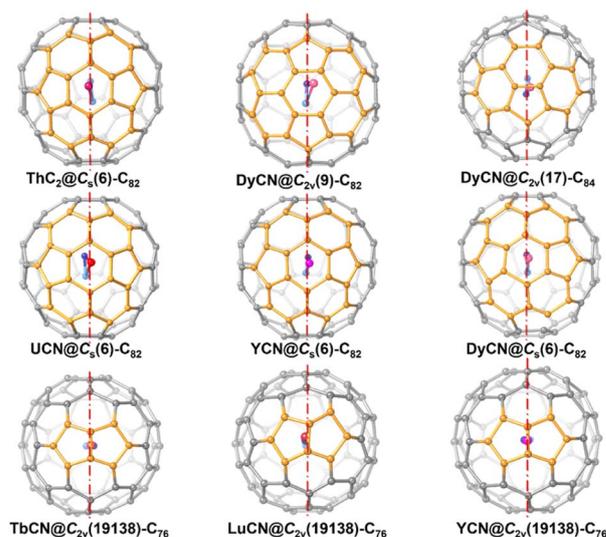

Fig. 4 Structures of crystallographically characterized mononuclear cluster fullerenes with pristine cages that contain symmetry planes (highlighted with dotted red lines). The fullerene cage segments closest to the encapsulated metal ions are highlighted in light orange.

a symmetry plane with the fullerene cages. That is, in general, as long as the fullerene encapsulating a mononuclear cluster possesses mirror planes, the entire molecule tends to be symmetric.

The identification of the encapsulated ThC_2 cluster expands our understanding of endohedral fullerenes. It represents a new type of endohedral cluster MC_2, in which a single metal ion is coordinated to a C≡C unit. In previous fullerene studies, if a fullerene compound was identified by mass spectrometry as MC_{2n}, it can be intuitively assigned as a mono-metallofullerene, i.e., $M@C_{2n}$, in which only a single metal ion is encapsulated inside the cage. The discovery of $MC_2@C_{2n}$, however, breaks this paradigm and suggests that MC_{2n} can also be the iso-structural isomer of $MC_2@C_{2n-2}$. Moreover, it provides the first crystallographic observation of a discrete ThC_2, which may be beneficial for the better understanding of those thorium carbide gas molecules generated in high temperature.

Fig. 3 Orbital isosurfaces (±0.03 au) and atomic orbital weight compositions (in %) obtained from NLMO analysis of the singlet ground state of $ThC_2@C_s(6)$–C_{82}.

Theoretical investigation

DFT calculations for $ThC_2@C_s(6)$–C_{82} and $ThC_2@C_2(5)$–C_{82} identified spin-singlet ground states. It is known that C_{82} can accept two electrons, for example, in the case of $Sm@C_{82}$ and $TbCN@C_{82}$ [$C_s(6)$ and $C_2(5)$ isomers].[46,47] Based on the frontier molecular orbitals in our calculations, we verified that there is a transfer of two electrons from the encapsulated ThC_2 cluster to the C_{82} cage, i.e., the system adopts a formal closed-shell $[Th^{4+}(C_2)^{2-}]^{2+}@[C_{82}]^{2-}$ electron configuration. Therefore, we interpret that $ThC_2@C_{82}$ isomers have similar two-electron transfer to those of $Sm@C_{82}$ and $TbCN@C_{82}$. In all three cases, isomeric structures of $C_s(6)$–C_{82} and $C_2(5)$–C_{82} are stabilized by the metal/cluster-to-cage two electron transfer.[46,47] For the spin-singlet states, the structural parameters optimized with the B3LYP hybrid functional match the experimental data
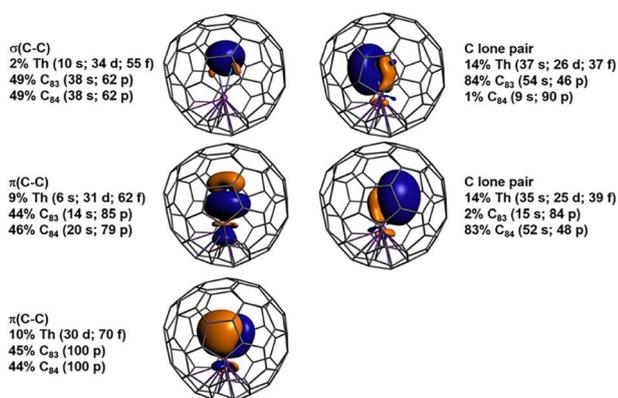
better than other tested functionals. The following discussion is based on all-electron scalar relativistic B3LYP optimizations and the corresponding electronic structures.

The metal–ligand bonding in $ThC_2@C_s(6)–C_{82}$ and $ThC_2@C_2(5)–C_{82}$, was characterized in terms of natural localized molecular orbitals (NLMOs) and Wiberg Bond Orders (WBOs). In $ThC_2@C_s(6)–C_{82}$, as shown in Fig. 3, there are three pairs of NLMOs, one σ and two π, describing the formal triple bond of C_2^{2-}. There is pronounced covalency with thorium. The two π NLMOs display three-center characteristics involving Th, with 10% and 9% weights of the orbital density associated with Th 6d–5f hybrids. The carbon lone pairs are even stronger donating, with 13% weight at thorium. The WBO for C_2^{2-} in the cluster fullerene is 2.51, that is, a triple bond slightly weakened by the donation to the metal. In comparison with other known Th–C bonds, the Th–C interaction in the fullerene shows double bond character. The average WBO of 0.85 is close to the bond order of 0.91 for the formal Th=C double bond in complex $[\{(NR_2)_3\}Th(CCCPh_2)]^-$ (R = $SiMe_3$)),[48] and nearly double the WBOs (0.47 and 0.49) of the single Th–C_{ipso} bonds in $[Li(DME)_2(Et_2O)]_2[Li(DME)_2][Th(C_6Cl_5)_5]_3$ and $[Li(DME)_2(Et_2O)][Li(Et_2O)_2][ThCl_3(C_6Cl_5)_3]$.[49] These data help rationalizing the aforementioned short Th–C distances. Some of the NLMOs centered in the fullerene also have density at Th; the corresponding plots are shown in Fig. S9.† Among them, the strongest Th–C(cage) interaction has 6% Th weight. Therefore, the formal transfer of two electrons from ThC_2 to C_{82} is accompanied by secondary cage-metal backbonding.

The main difference between $ThC_2@C_2(5)–C_{82}$ and $ThC_2@C_s(6)–C_{82}$ (Fig. S8 and S10†) is the backbonding between Th and the fullerene, with only 4% for the largest Th weight in the former, which may rationalize the slightly higher energy of $ThC_2@C_2(5)–C_{82}$ by 2 kcal mol^{-1}.

Spectroscopic characterization

The UV–vis–NIR absorption spectra of $ThC_2@C_s(6)–C_{82}$ and $ThC_2@C_2(5)–C_{82}$ dissolved in CS_2 are shown in Fig. 5.
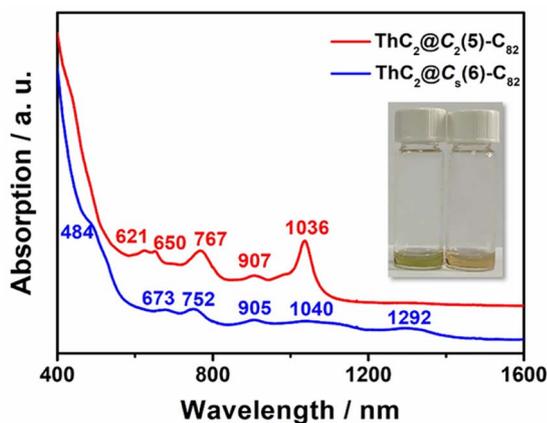

Fig. 5 UV–vis–NIR spectra of $ThC_2@C_s(6)–C_{82}$ and $ThC_2@C_2(5)–C_{82}$ dissolved in CS_2. Insets: Photographs of $ThC_2@C_2(5)–C_{82}$ (left) and $ThC_2@C_s(6)–C_{82}$ (right) dissolved in CS_2.

$ThC_2@C_s(6)–C_{82}$ shows broad peaks at 673, 752, 905, 1040, and 1292 nm and a shoulder peak at 484 nm, similar to those of $TbCN@C_s(6)–C_{82}$.[46] For $ThC_2@C_2(5)–C_{82}$, the characteristic absorption peaks were observed at 621, 650, 767, 907, and 1036 cm^{-1}, almost identical to those of $TbCN@C_2(5)–C_{82}$ with the same fullerene cage.[46] This indicates similar cage isomer and electronic transfer between $ThC_2@C_{82}(C_s(6)$ and $C_2(5))$ and $TbCN@C_{82}(C_s(6)$ and $C_2(5))$, which is consistent with the results obtained from single-crystal X-ray diffraction and the computational results for $[ThC_2]^{2+}@C_{82}^{2-}$.

Conclusions

For the first time, thorium clusters were encapsulated inside fullerene cages. $ThC_2@C_s(6)–C_{82}$ and $ThC_2@C_2(5)–C_{82}$ were synthesized and characterized by mass spectrometry, single-crystal X-ray diffraction crystallography, UV–vis–NIR spectroscopy and DFT calculations. Crystallographic studies reveal that a mononuclear carbide, which has never been found in endohedral fullerenes, is stabilized inside a C_{82} cage. The two Th–C bond lengths of the ThC_2 cluster encapsulated in both $C_s(6)–C_{82}$ and $C_2(5)–C_{82}$ are 2.360(11)/2.353(10) Å and 2.334(15)/2.385(14) Å, presenting isosceles triangular configurations, although the latter shows slight distortion, likely affected by the different cage isomeric structures.

DFT calculations for two isomers of $ThC_2@C_{82}$ revealed that the electronic structure can be described as a spin singlet ground state, formally $[Th^{4+}(C_2)^{2-}]^{2+}@[C_{82}]^{2-}$, with pronounced donation bonding from $(C_2)^{2-}$ to Th^{4+} and secondary backbonding from the fullerene to thorium. The triangular cluster $[ThC_2]^{2+}$ is more stable in the $C_s(6)–C_{82}$ cage (**1a**) than in the $C_2(5)–C_{82}$ cage (**2a**), which is in part rationalized by a weaker backbonding in the latter. Theoretical analysis also shows a triple bond in the C_2^{2-} fragment that is somewhat weakened by the donation to the metal. The calculations provide an intuitive description of the bonding of actinide and main group atoms as they are encapsulated in fullerenes.

This work expands the scope of both endohedral fullerenes and actinide compounds. $ThC_2@C_{82}$ represents a new family of endohedral fullerenes, which reveals for the first time that MC_{2n} fullerenes, the most commonly observed endohedral fullerenes, may have two isomeric structures, namely, $M@C_{2n}$ *versus* $MC_2@C_{2n-2}$. Furthermore, identification of the unique bonding motif of ThC_2 deepens our understanding of the chemical bonding of thorium.

Experimental section

Spectroscopic study

Positive-ion mode matrix-assisted laser desorption ionization time-of-flight (MALDI-TOF) (Bruker, Germany) was employed for mass characterization. The UV–vis–NIR spectra of the purified $ThC_2@C_{82}$ were measured in CS_2 solution with a Cary 5000 UV–vis–NIR spectrophotometer (Agilent, USA).

X-ray crystallographic study

The black block crystals of $ThC_2@C_s(6)–C_{82}$ and $ThC_2@C_2(5)–C_{82}$ were obtained by slow diffusion of the CS_2 solution of the corresponding metallofullerene compounds into the benzene solution of $[Ni^{II}(OEP)]$. Single-crystal X-ray data of $ThC_2@C_s(6)–C_{82}$ and $ThC_2@C_2(5)–C_{82}$ were collected at 120 K on a diffractometer (Bruker D8 Venture) equipped with a CCD collector. The multiscan method was used for absorption correction. The structures were solved using direct methods[50] and refined on F^2 using full-matrix least-squares using the SHELXL2015 crystallographic software packages.[51] Hydrogen atoms were inserted at calculated positions and constrained with isotropic thermal parameters. Crystal data for $ThC_2@C_s(6)–C_{82}·[Ni^{II}(OEP)]·2C_6H_6$ and $ThC_2@C_2(5)–C_{82}·[Ni^{II}(OEP)]·2C_6H_6$ are provided in Table S4.†

Computational details

Kohn–Sham density functional calculations were performed for $ThC_2@C_s(6)–C_{82}$ and $ThC_2@C_2(5)–C_{82}$ structures with the 2017 release of the Amsterdam Density Functional (ADF) suite.[52] Different functionals, including the Perdew–Burke–Ernzerhof (PBE) and Becke–Perdew (BP86) nonhybrid functional, a global hybrid based on PBE with 25% exact exchange (PBE0), and the popular B3LYP hybrid functionals, were used in conjunction with all-electron Slater-type atomic orbital (STO) basis sets of triple-ζ polarized (TZP) quality for the geometry optimizations and electronic structure analyses.[53–58] Relativistic effects were considered by means of the scalar-relativistic Zeroth-Order Regular Approximation (ZORA) Hamiltonian.[59] An atom-pairwise correction for dispersion forces was considered *via* Grimme's D3 model augmented with Becke–Johnson (BJ) damping.[60] To quantify the compositions of the chemical bonds for selected optimized systems, natural localized molecular orbital (NLMO) analyses were carried out with the NBO program, version 6.0, interfaced with ADF.[61]

Data availability

CCDC 2183932 and 2183933 contain the supplementary crystallographic data for this paper.† These data can be obtained free of charge *via* **https://www.ccdc.cam.ac.uk/data_request/cif**. All other data supporting the findings of this study are available from the corresponding authors on request.

Author contributions

N. C. conceived and designed the experiments. Y. S. and Q. M. synthesized and isolated all the compounds. J. A. and X. Y. performed the computations and theoretical analyses. Y. S. and Q. M. performed the single-crystal measurements. Y. Y. and Y. S. performed the crystallographic analysis. Y. S. performed the spectroscopic measurements. N. C., J. A., Y. S., X. Y., Q. M. and Y. Y. co-wrote the manuscript.

Conflicts of interest

There are no conflicts to declare.

Acknowledgements

Notes and references

1 A. A. Popov, S. Yang and L. Dunsch, *Chem. Rev.*, 2013, **113**, 5989–6113.

2 S. Yang, T. Wei and F. Jin, *Chem. Soc. Rev.*, 2017, **46**, 5005–5058.

3 W. Shen, S. Hu and X. Lu, *Chem.–Eur. J.*, 2020, **26**, 5748–5757.

4 G. Velkos, W. Yang, Y. R. Yao, S. M. Sudarkova, X. Liu, B. Buchner, S. M. Avdoshenko, N. Chen and A. A. Popov, *Chem. Sci.*, 2020, **11**, 4766–4772.

5 F. Liu, S. Wang, C.-L. Gao, Q. Deng, X. Zhu, A. Kostanyan, R. Westerström, F. Jin, S.-Y. Xie, A. A. Popov, T. Greber and S. Yang, *Angew. Chem., Int. Ed.*, 2017, **56**, 1830–1834.

6 T. Li, S. Murphy, B. Kiselev, K. S. Bakshi, J. Zhang, A. Eltahir, Y. Zhang, Y. Chen, J. Zhu, R. M. Davis, L. A. Madsen, J. R. Morris, D. R. Karolyi, S. M. LaConte, Z. Sheng and H. C. Dorn, *J. Am. Chem. Soc.*, 2015, **137**, 7881–7888.

7 W. Li, F. Qu, L. Liu, Z. Zhang, J. Liang, Y. Lu, J. Zhang, L. Wang, C. Wang and T. Wang, *Angew. Chem., Int. Ed.*, 2022, **61**, e202116854.

8 F. Liu, L. Spree, D. S. Krylov, G. Velkos, S. M. Avdoshenko and A. A. Popov, *Acc. Chem. Res.*, 2019, **52**, 2981–2993.

9 X. Zhang, W. Li, L. Feng, X. Chen, A. Hansen, S. Grimme, S. Fortier, D. C. Sergentu, T. J. Duignan, J. Autschbach, S. Wang, Y. Wang, G. Velkos, A. A. Popov, N. Aghdassi, S. Duhm, X. Li, J. Li, L. Echegoyen, W. H. E. Schwarz and N. Chen, *Nat. Commun.*, 2018, **9**, 2753.

10 J. Zhuang, L. Abella, D. C. Sergentu, Y. R. Yao, M. Jin, W. Yang, X. Zhang, X. Li, D. Zhang, Y. Zhao, X. Li, S. Wang, L. Echegoyen, J. Autschbach and N. Chen, *J. Am. Chem. Soc.*, 2019, **141**, 20249–20260.

11 Q. Meng, L. Abella, W. Yang, Y. R. Yao, X. Liu, J. Zhuang, X. Li, L. Echegoyen, J. Autschbach and N. Chen, *J. Am. Chem. Soc.*, 2021, **143**, 16226–16234.

12 X. Lu, T. Akasaka and S. Nagase, *Acc. Chem. Res.*, 2013, **46**, 1627–1635.

13 P. Bagla, *Science*, 2015, **350**, 726–727.

14 T. Abram and S. Ion, *Energy Policy*, 2008, **36**, 4323–4330.

15 D. R. J. Konings, T. R. Allen, R. E. Stoller and P. S. Yamanaka, *Technical Report*, Oak Ridge National Laboratory (ORNL), 2012.

16 H. Kleykamp, Thorium Carbides, in *Gmelin Handbook of Inorganic and Organometallic Chemistry*, 8th edn, Springer, Berlin, Germany, 1992, vol. C6.

17 R. J. Needs and C. J. Pickard, *APL Mater.*, 2016, **4**, 053210.

18 P. Pogany, A. Kovacs, Z. Varga, F. M. Bickelhaupt and R. J. Konings, *J. Phys. Chem. A*, 2012, **116**, 747–755.

19 K. A. Cingerich, *Chem. Phys. Lett.*, 1978, **59**, 136–139.

20 D. D. Jackson, G. W. Barton, O. H. Krikorian and R. S. Newbury, *J. Phys. Chem.*, 1964, **68**, 1516–1523.

21 N. Sasaki, K. Kubo and M. Asano, *J. Nucl. Sci. Technol.*, 1971, **8**, 614–621.

22 S. K. Gupta and K. A. Gingerich, *J. Chem. Phys.*, 1980, **72**, 2795–2800.

23 I. R. Shein and A. L. Ivanovskii, *J. Nucl. Mater.*, 2009, **393**, 192–196.

24 D. W. Jones, I. J. McColm, R. Steadman and J. Yerkess, *J. Solid State Chem.*, 1987, **68**, 219–226.

25 A. L. Bowman, N. H. Krikorian, G. P. Arnold, T. C. Wallace and N. G. Nereson, *Acta Crystallogr., Sect. B: Struct. Crystallogr. Cryst. Chem.*, 1968, **24**, 1121–1123.

26 I. R. Shein, K. I. Shein, N. I. Medvedeva and A. L. Ivanovskii, *Phys. Status Solidi*, 2007, **244**, 3198–3205.

27 C.-R. Wang, T. Kai, T. Tomiyama, T. Yoshida, Y. Kobayashi, E. Nishibori, M. Takata, M. Sakata and H. Shinohara, *Angew. Chem., Int. Ed.*, 2001, **40**, 397–399.

28 Y. Iiduka, T. Wakahara, K. Nakajima, T. Tsuchiya, T. Nakahodo, Y. Maeda, T. Akasaka, N. Mizorogi and S. Nagase, *Chem. Commun.*, 2006, 2057–2059.

29 X. Lu, K. Nakajima, Y. Iiduka, H. Nikawa, N. Mizorogi, Z. Slanina, T. Tsuchiya, S. Nagase and T. Akasaka, *J. Am. Chem. Soc.*, 2011, **133**, 19553–19558.

30 X. Lu, K. Nakajima, Y. Iiduka, H. Nikawa, T. Tsuchiya, N. Mizorogi, Z. Slanina, S. Nagase and T. Akasaka, *Angew. Chem., Int. Ed.*, 2012, **51**, 5889–5892.

31 J. Zhang, F. L. Bowles, D. W. Bearden, W. K. Ray, T. Fuhrer, Y. Ye, C. Dixon, K. Harich, R. F. Helm, M. M. Olmstead, A. L. Balch and H. C. Dorn, *Nat. Chem.*, 2013, **5**, 880–885.

32 W. Shen, L. Bao, P. Yu, L. Yang, B. Li, P. Yu, P. Jin and X. Lu, *Carbon*, 2020, **164**, 157–163.

33 Y. Iiduka, T. Wakahara, T. Nakahodo, T. Tsuchiya, A. Sakuraba, Y. Maeda, T. Akasaka, K. Yoza, E. Horn, T. Kato, M. T. H. Liu, N. Mizorogi, K. Kobayashi and S. Nagase, *J. Am. Chem. Soc.*, 2005, **127**, 12500–12501.

34 Y. R. Yao, Y. Rosello, L. Ma, A. R. Puente Santiago, A. Metta-Magana, N. Chen, A. Rodriguez-Fortea, J. M. Poblet and L. Echegoyen, *J. Am. Chem. Soc.*, 2021, **143**, 15309–15318.

35 C. N. Carlson, T. P. Hanusa and W. W. Brennessel, *J. Am. Chem. Soc.*, 2004, **126**, 10550–10551.

36 K. C. Jantunen, C. J. Burns, I. Castro-Rodriguez, R. E. Da Re, J. T. Golden, D. E. Morris, B. L. Scott, F. L. Taw and J. L. Kiplinger, *Organometallics*, 2004, **23**, 4682–4692.

37 Y. Wang, Q. Tang, L. Feng and N. Chen, *Inorg. Chem.*, 2017, **56**, 1974–1980.

38 H. Yang, C. Lu, Z. Liu, H. Jin, Y. Che, M. M. Olmstead and A. L. Balch, *J. Am. Chem. Soc.*, 2008, **130**, 17296–17300.

39 C. Zhang, G. Hou, G. Zi, W. Ding and M. D. Walter, *J. Am. Chem. Soc.*, 2018, **140**, 14511–14525.

40 C. Zhang, G. Hou, G. Zi, W. Ding and M. D. Walter, *Inorg. Chem.*, 2019, **58**, 1571–1590.

41 P. Tecmer, K. Boguslawski and P. W. Ayers, *Phys. Chem. Chem. Phys.*, 2015, **17**, 14427–14436.

42 S. Yang, C. Chen, F. Liu, Y. Xie, F. Li, M. Jiao, M. Suzuki, T. Wei, S. Wang, Z. Chen, X. Lu and T. Akasaka, *Sci. Rep.*, 2013, **3**, 1487.

43 J. Xin, F. Jin, R. Guan, M. Chen, X.-M. Xie, Q. Zhang, S.-Y. Xie and S. Yang, *Inorg. Chem. Front.*, 2021, **8**, 1719–1726.

44 W. Shen, Z. Hu, P. Yu, Z. Wei, P. Jin, Z. Shi and X. Lu, *Inorg. Chem. Front.*, 2020, **7**, 4563–4571.

45 R. Guan, M. Chen, J. Xin, X.-M. Xie, F. Jin, Q. Zhang, S.-Y. Xie and S. Yang, *J. Am. Chem. Soc.*, 2021, **143**, 8078–8085.

46 F. Liu, C. L. Gao, Q. Deng, X. Zhu, A. Kostanyan, R. Westerstrom, S. Wang, Y. Z. Tan, J. Tao, S. Y. Xie, A. A. Popov, T. Greber and S. Yang, *J. Am. Chem. Soc.*, 2016, **138**, 14764–14771.

47 H. Yang, H. Jin, X. Wang, Z. Liu, M. Yu, F. Zhao, B. Q. Mercado, M. M. Olmstead and A. L. Balch, *J. Am. Chem. Soc.*, 2012, **134**, 14127–14136.

48 G. T. Kent, X. Yu, G. Wu, J. Autschbach and T. W. Hayton, *Chem. Sci.*, 2021, **12**, 14383–14388.

49 O. Ordoñez, X. Yu, G. Wu, J. Autschbach and T. W. Hayton, *Inorg. Chem.*, 2021, **60**, 12436–12444.

50 O. V. Dolomanov, L. J. Bourhis, R. J. Gildea, J. A. K. Howard and H. Puschmann, *J. Appl. Crystallogr.*, 2009, **42**, 339–341.

51 G. Sheldrick, *Acta Crystallogr., Sect. C: Struct. Chem.*, 2015, **71**, 3–8.

52 E. J. Baerends, T. Ziegler, A. Atkins, J. Autschbach, D. Bashford, O. Baseggio, A. Bérces, F. Bickelhaupt, C. Bo and P. Boerritger. *ADF2017, SCM, Theoretical Chemistry*, Vrije University, Amsterdam, The Netherlands, 2017.

53 J. P. Perdew, *Phys. Rev. B: Condens. Matter Mater. Phys.*, 1986, **34**, 7406.

54 J. P. Perdew, J. A. Chevary, S. H. Vosko, K. A. Jackson, M. R. Pederson, D. J. Singh and C. Fiolhais, *Phys. Rev. B*, 1992, **46**, 6671–6687.

55 A. D. Becke, *J. Chem. Phys.*, 1986, **85**, 7184–7187.

56 A. D. Becke, *Phys. Rev. A*, 1988, **38**, 3098–3100.

57 C. Lee, W. Yang and R. G. Parr, *Phys. Rev. B: Condens. Matter Mater. Phys.*, 1988, **37**, 785–789.

58 E. van Lenthe and E. J. Baerends, *J. Comput. Chem.*, 2003, **24**, 1142–1156.

59 E. van Lenthe, E. J. Baerends and J. G. Snijders, *J. Chem. Phys.*, 1993, **99**, 4597–4610.

60 S. Grimme, S. Ehrlich and L. Goerigk, *J. Comput. Chem.*, 2011, **32**, 1456–1465.

61 E. D. Glendening, C. R. Landis and F. Weinhold, *J. Comput. Chem.*, 2013, **34**, 1429–1437.